

Nanorheology of Confined Polymer Melts. 3. Weakly Adsorbing Surfaces

John Peanasky, Lenore L. Cai, and Steve Granick*

Materials Research Laboratory and Department of Materials Science and Engineering,
University of Illinois, Urbana, Illinois 61801

Carl R. Kessel

Adhesive Technologies Center, 3M Company, 201-4N-01, 3M Center,
St. Paul, Minnesota 55144

Received December 13, 1993. In Final Form: July 27, 1994[⊗]

Polymer melts confined between weakly adsorbing surfaces terminated with methyl groups (close-packed self-assembled monolayers of condensed octadecyltriethoxysilane, OTE) were studied in regard to surface forces (static forces to compress the polymer films to a given thickness) and shear rheology. The experiments involved a surface force apparatus modified for dynamic mechanical shear oscillation. The polymers were an atactic poly(phenylmethylsiloxane), PPMS, with chain length from 31 to 153 skeletal bonds. Three principal conclusions emerged. First, the equilibrated surface force between OTE was zero down to the same small thickness (17 ± 2 Å) regardless of molecular weight. This decisively confirms theoretical predictions for the surface forces of polymer chains in equilibrium with a bulk reservoir. Second, enhanced effective shear moduli (measured in the linear-response regime) were observed only at this thickness of measurable surface force. This accompaniment of surface force and enhanced shear modulus was also seen in the case of strong adsorption. But in that case, these phenomena scaled with the molecular size of the polymer, approximately its radius of gyration (R_G); here these phenomena appeared at a single film thickness. Third, the effective elastic shear modulus G' under confinement was rubberlike in magnitude, indicating enormously slower relaxation than in the bulk fluid. This relaxation was slower, the higher the polymer molecular weight. This third conclusion is qualitatively similar to the case for these same PPMS polymers confined between strongly adsorbing surfaces. It suggests that, even in the case of weak adsorption, geometrical confinement enhances entanglement interactions between polymer chains.

Introduction

A burgeoning literature concerned with the near-surface statics and dynamics of polymers—but at adsorbing surfaces—has made clear the prominence of long-lived nonequilibrium dynamical structures. Examples of unexpectedly slow surface mobility concern the spreading of polymer melts,¹ the adsorption-desorption dynamics of polymers in solution,² surface forces,³⁻⁸ and nanorheology.^{7,8} We consider in this paper the problem of surface forces. In response to a momentary repulsion, confined polymers would migrate out of the intersurface region and dissipate this repulsion if equilibrium could be attained.⁹⁻¹² Experimentally, however, persistent strong repulsion has been observed starting when the films are thick, several times the unperturbed radius of gyration,³⁻⁸ and dynamic experiments also indicate a spectacular slowing down of near-surface dynamics.^{7,8} Outside the

context of a few experiments at the solid-air interface which involve spreading or dewetting,^{1,13,14} all of the experimental studies have involved polymers confined between surfaces that were completely wet by the polymer.

Therefore, on the basis of work done to date, it is difficult to assess the respective effects of geometrical confinement, and of strong surface adsorption, in these studies. Indeed, the prominent consequences of adsorption, and the difficulty of meeting full equilibrium conditions, can be appreciated by considering the adsorption per segment of a nonpolar liquid onto a strongly adsorbing surface, mica, approximately $3-5k_B T^{15}$ (k_B is the Boltzmann constant, and T is the absolute temperature). This must be added up over approximately $N^{1/2}$ adsorbed contacts, where N is the degree of polymerization. The prominent effects of adsorption on polymer interfacial properties is also suggested by computer simulations¹⁷⁻²⁰ and liquid-state calculations.¹⁵

Here, for the first time, experiments are presented of surface forces and shear rheology of polymer melts confined between surfaces to which the adsorption was weak. Tentative conclusions are drawn regarding the respective importance of adsorption and of geometrical confinement.

[⊗] Abstract published in *Advance ACS Abstracts*, September 15, 1994.

(1) Silberzan, P.; Léger, L. *Macromolecules* **1992**, *25*, 1267 and references therein.

(2) Granick, S. In *Physics and Chemistry of Polymer Surfaces*; Sanchez, I., Ed.; Butterworth-Heinemann: Boston, 1992; and references therein.

(3) Montfort, J. P.; Hadziioannou, G. *J. Chem. Phys.* **1988**, *88*, 7187.

(4) Horn, R. G.; Israelachvili, J. N. *Macromolecules* **1988**, *21*, 2836.

(5) Horn, R. G.; Hirz, S. J.; Hadziouannou, G.; Frank, C. W.; Catala, J. M. *J. Chem. Phys.* **1989**, *90*, 6767.

(6) Israelachvili, J. N.; Kott, S. J.; Fetters, L. J. *J. Polym. Sci. Polym. Phys. Ed.* **1989**, *27*, 489.

(7) Van Alsten, J.; Granick, S. *Macromolecules* **1990**, *23*, 4856.

(8) Hu, H.-W.; Granick, S. *Science* **1992**, *258*, 1339.

(9) de Gennes, P.-G. *C. R. Acad. Sci. Paris* **1987**, *305*, 1181.

(10) de Gennes, P.-G. In *Liquids at Interfaces*; Charvolin, J.; Joanny, J. F.; Zinn-Justin, J., Eds. Elsevier: Amsterdam, 1990; Les Houches, Session XLVIII.

(11) Brinke, G. T.; Auseré, D.; Hadziioannou, G. *J. Chem. Phys.* **1988**, *89*, 4374.

(12) For a review, see: Auseré, D. *J. Phys. Fr.* **1989**, *50*, 3021.

(13) Reiter, G. *Phys. Rev. Lett.* **1991**, *68*, 75.

(14) Zhao, W.; Rafailovich, H.; Sokolov, J.; Fetters, L. J.; Plano, R.; Sanyal, M. K.; Sinha, S. K.; Sauer, B. B. *Macromolecules* **1993**, *70*, 1453.

(15) Hu, H.-W.; Granick, S.; Schweizer, K. S. *J. Noncryst. Solids*, in press.

(16) Thompson, P. A.; Grest, G. S.; Robbins, M. O. *Phys. Rev. Lett.* **1992**, *68*, 3448.

(17) Mansfield, K. F.; Theodorou, D. N. *Macromolecules* **1989**, *22*, 3143.

(18) Bitsanis, I. A.; Hadziioannou, G. *J. Chem. Phys.* **1990**, *92*, 3287.

(19) Bitsanis, I. A.; Pan, C. *J. Chem. Phys.* **1993**, *99*, 5520.

(20) Gupta, S.; Koopman, D. C.; Westermann-Clark, G. B.; Bitsanis, I. A. Preprint.

Table 1. Molecular Characteristics of the PPMS Samples

code	M_n^a (g mol ⁻¹)	M_w/M_n^b	n_n^c	R_G^d (Å)
polymer A	2240	1.08	31	9
polymer B	4550	1.14	65	13
polymer C	10600	1.16	153	20
polymer D	19500	1.12	284	26

^a Number-average molecular weight. ^b Ratio of weight-average to number-average molecular weight. ^c Number-average number of skeletal bonds. ^d Unperturbed radius of gyration, estimated from the chain length by a rotational isomeric states calculation.²⁵

Experimental Section

Self-Assembled Monolayers on Mica. The protocol to coat a freshly-cleaved mica surface with a securely-attached, self-assembled organic monolayer is described elsewhere.^{21,22} The chemistry involves the condensation of hydrolyzed octadecyltriethoxysilane (OTE). The packing density and degree of crystallinity of the octadecyl alkane chains in the resulting monolayer are comparable in quality to a LB (Langmuir-Blodgett) film of barium stearate.²¹

In these films, the close-packed chains terminate with methyl groups. In films of similar quality, X-ray diffraction and helium scattering indicate that the methyl groups are amorphous over distances greater than 50–100 Å;²² the surface should not guide an epitaxial crystallization of the surrounding liquid. In addition, the surface energy is only ≈ 21 mJ m⁻²,²¹ considerably less than the 200–400 mJ m⁻² typical of freshly-cleaved mica, so substantially weaker coupling to the surface is expected than in the case of mica. This is confirmed by measurements of the finite contact angle of PPMS on OTE, noted below.

The thickness of two OTE monolayers, in van der Waals adhesion, is 51 ± 3 Å relative to mica–mica contact.²² This thickness was measured separately in each experiment. Whenever possible, the OTE thickness and the polymer force–distance profiles were measured at the same spot. As the polymer film thickness was calculated by subtracting the OTE thickness from the measured mica–mica separation, this served to minimize uncertainties regarding polymer film thickness associated with the propagation of errors.

Polymers. The polymer fluids, atactic methyl-terminated poly(phenylmethylsiloxane) (PPMS),^{23,24} were generously donated by S. J. Clarson of the University of Cincinnati. These are amorphous and flexible chains with a low bulk glass transition temperature ($T_g \approx -30$ °C). The temperature of the experiments was 26 ± 0.5 °C.

Molecular characteristics of the samples studied are given in Table 1. The unperturbed radius of gyration (R_G) was estimated from the chain length by a rotational isomeric states calculation.²⁵ The persistence length of atactic PPMS in the bulk, estimated from the characteristic ratio, is about 6 skeletal bonds.²⁵

Although we have no direct measurement of the entanglement length of PPMS (because of a limited amount of sample), from the calculated chain stiffness²⁵ one expects that the molecular weight between entanglements is $M_e \approx 12\,000$ g mol⁻¹,²⁶ so that chains of the length studied here would be too short to be entangled in the bulk.

In the interaction of PPMS with mica, a conservative estimate of the adsorption strength is $3-5k_B T$ per repeat unit¹⁵ (k_B is the Boltzmann constant, and T is the absolute temperature). To test this estimate, control experiments (in which PPMS was displaced from mica by water) showed that adsorption was reversible. As would be expected, the polymers wet mica completely with contact angles of zero degrees.

Based on the difference in surface energy between bare mica and OTE, a conservative estimate of the adsorption strength is

(21) Kessel, C.; Granick, S. *Langmuir* **1991**, *7*, 532.

(22) Peanasky, J.; Schneider, H. M.; Granick, S.; Kessel, C. Submitted for publication.

(23) Clarson, S. J.; Dodgson, K.; Semlyen, J. A. *Polymer* **1987**, *28*, 189.

(24) Clarson, S. J.; Semlyen, J. A.; Dodgson, K. *Polymer* **1991**, *32*, 2823.

(25) Mark, J. E.; Ko, J. H. *J. Polym. Sci. Polym. Phys. Ed.* **1975**, *13*, 2221.

(26) Aharoni, S. M. *Macromolecules* **1983**, *16*, 1722.

$<3-5k_B T$ per repeat unit. As expected, the contact angle of these polymers against OTE-coated mica was 40° , indicating¹ a state of partial wetting.

Surface Forces and Dynamic Measurements. The experimental apparatus^{27,28} and protocol^{29,30} are reported in detail elsewhere. In brief, the polymer fluids were confined between atomically smooth, step-free single crystals of muscovite mica, coated with OTE monolayers, surrounded by a droplet reservoir.^{27,28} To measure shear forces, a sinusoidal time-varying shear force was applied, and the amplitude and phase of response were measured. The small influence of mechanical deformation within the device was accounted for by a model in which the calibrated properties of the device acted in parallel with the thin film.^{8,30} Recent improvements have increased the system resolution and stability so that viscous forces as low as 10^{-9} N are resolved. Control experiments with shear amplitudes as low as 0.5 Å confirmed that the response was linear in amplitude over the frequencies studied, 0.02–260 Hz.

The in-phase and out-of-phase shear forces as a function of radian frequency, ω , were calculated by conventional methods.³¹ In this calculation the strain is defined, for reasons discussed previously,⁸ to be deflection amplitude divided by film thickness. In this paper, the measurements of shear rheology were made at low peak deflection amplitudes, 2–10 Å. Control experiments verified that this was in the regime of linear viscoelastic response.

In contrast to the parallel plate geometry previously employed by this laboratory to investigate the shear of PPMS between mica (strongly adsorbing) surfaces,^{8,30} many of the measurements in this study were made between smoothly curved crossed cylinders. In general, we have found it more difficult to produce parallel plate geometry between OTE-coated surfaces than between mica surfaces. This difficulty is probably related to experimental conditions such as the amount of glue used to attach the mica sheet to the glass lens, but we cannot rule out the possibility that there is an intrinsic difference in flattening of the surfaces, in response to pressure, when the mica is coated with OTE. Implications of this difference in geometry are discussed below in connection with Figures 9 and 10, with the conclusion that the data are qualitatively comparable.

The rheology of the OTE layer itself was calibrated in the course of the usual glue and device calibrations,³⁰ by placing OTE layers into adhesive contact in dry air. Corrections for deflection within the OTE layer itself were insignificant.

Results and Discussion

Compressive Surface Forces. First we contrast the forces to compress films of the polymer samples to a specified thickness between OTE-coated mica (weakly adsorbing) and between mica (strongly adsorbing). Theoretically, zero force is expected if polymers in the gap between the two solids are in equilibrium with polymers outside the gap.^{9–12}

The respective force–distance profiles measured for polymer C during compression are shown in Figure 1. There is an obvious qualitative difference between these two sets of data. In the case of mica, the surface forces rose monotonically, starting at thickness $D < 5-6R_G$ (100–120 Å), consistent with our earlier findings for a polymer of lower molecular weight.⁸

This contrasts so strongly with the theoretical predictions^{9–12} that the question of equilibration becomes an essential point. However, the equilibration time was varied from 20 min to 24 h per datum, with no discernible effect, which implies that equilibration demanded times much longer times than hours.⁸ These nonequilibrium forces may result because molecules were pinned to the adsorbing surface by adsorption and then entropically

(27) Van Alsten, J.; Granick, S. *Phys. Rev. Lett.* **1988**, *61*, 2570.

(28) Peachey, J.; Van Alsten, J.; Granick, S. *Rev. Sci. Instrum.* **1991**, *62*, 463.

(29) Hu, H.-W.; Granick, S. *Macromolecules* **1990**, *23*, 613.

(30) Granick, S.; Hu, H.-W. Accompanying paper.

(31) For a review, see: Ferry, J. D. *Viscoelastic Properties of Polymers*, 3rd ed.; Wiley: New York, 1980.

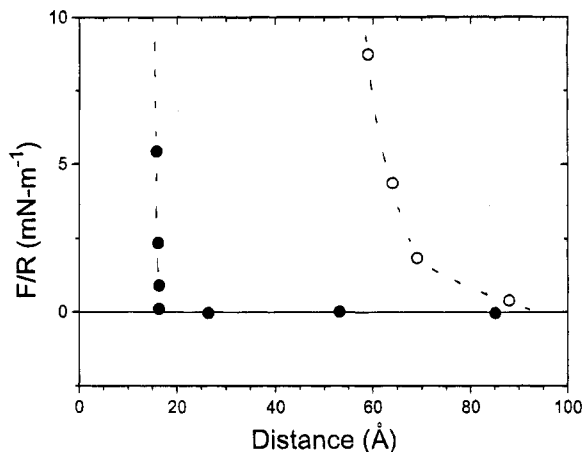


Figure 1. Contrast of the force–distance profiles upon compressing polymer C between a strongly adsorbing surface (bare mica, hollow circles) and between a surface not wet by the polymer (OTE surfaces, filled circles). Force is normalized by radius of curvature, R , of the crossed mica cylinders. Distance scale indicates thickness of the polymer film. The polymer radius of gyration is ≈ 20 Å as discussed in the text.

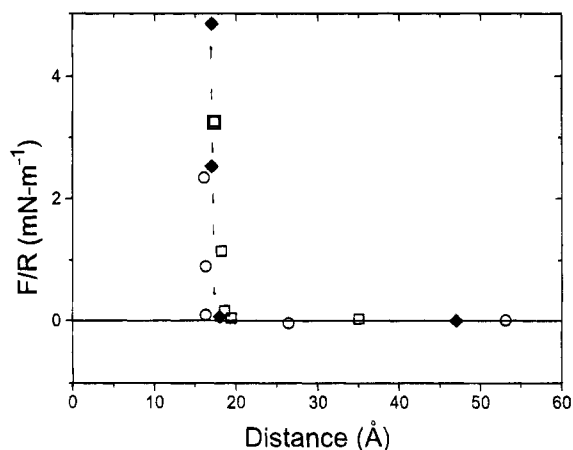


Figure 2. Comparison of the force–distance profiles upon compressing polymer A (diamonds), polymer B (squares), and polymer C (circles) between OTE surfaces. Force is normalized by radius of curvature, R , of the crossed mica cylinders. Distance scale indicates thickness of the polymer film.

deformed by the compression.^{9,10,30} Alternative possibilities have also been discussed.¹⁵

The new result in Figure 1 is the evident absence, for PPMS between OTE-coated mica, of this long-range repulsion. No force was required to compress polymer C down to 17 ± 2 Å. Recall that the film thickness in these measurements is defined relative to the thickness of the OTE films in van der Waals adhesive contact in air. This thickness, measured separately in each experiment, was subtracted from the measured mica–mica separation. It is also worth noting that this equilibration was achieved over rather short time periods—at most 30 min per datum. In response to a momentary repulsion resulting from a step increase in compressive force, the confined polymers migrated out of the intersurface region and dissipated this repulsion.

When the molecular weight was varied, this conclusion continued to hold. The normalized forces to compress polymer A, polymer B, and polymer C between OTE-coated mica are plotted in Figure 2. It is obvious that these data are indistinguishable: zero force down to 17 ± 2 Å, followed by a zone of extremely steep and almost vertical repulsion. The point of repulsion, effectively a “hard wall”, was independent of molecular weight. We emphasize that this

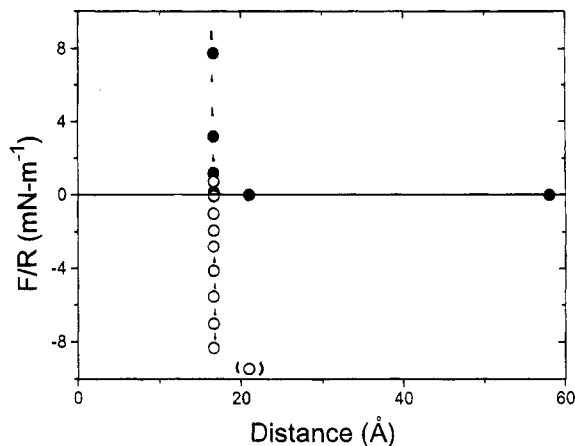


Figure 3. Attractive forces measured upon separating compressed film of polymer A. Force is normalized by radius of curvature, R , of the crossed mica cylinders. Equilibration per point: 5 min upon compression (filled circles), 10 min upon separation (hollow circles).

was observed despite the significant differences in estimated radius of gyration, R_G (cf. Table 1). This contrasts acutely with the finding for these same polymers confined between bare mica, that normal forces grow in proportion to film thickness scaled by R_G .^{8,30}

These findings decisively corroborate the theoretical expectation, long predicted^{9–12} but not to our knowledge observed previously,^{3–8} regarding surface forces of polymer in equilibrium with a bulk reservoir. For polymers in equilibrium with a bulk reservoir, one should not see surface forces until the plate separation is on the order of the monomer thickness.

Adhesion upon Separation. The strong adhesive forces upon separating the films from the point of hard-wall repulsion were unusually slow to equilibrate. The data for polymer A, plotted in Figure 3 and obtained with an equilibration time of 10 min per datum, show a fairly large adhesion of ≈ -9 mN m⁻¹.

This general level of adhesion, at this film thickness, is typical of that for structural forces of small molecules between mica,³² except that (as we discussed below) adhesion was measurable from only this sole thickness. Structural forces are analogous to the radial density distribution function of molecules in the isotropic bulk; they reflect density oscillations of liquid in the direction normal to two solid surfaces.³²

However, in contrast to the present observations, in small-molecule systems the attraction oscillates with repulsion as the film thickness changes, with periodicity of a segmental dimension, and the liquid films display adhesion at several discrete film thicknesses.³² To test the generality of this view for small-molecule liquids confined between OTE, control experiments were performed with undecane (Fluka, >99.5% pure). The contact angle of undecane on OTE is 33° , similar to that for PPMS on OTE (see above). Figure 4 compares the force–distance profiles of undecane between bare mica and between OTE. The data clearly show layering for this simple alkane—an oscillation of adhesive forces, with periodicity roughly the thickness of the methylene chain. By analogy, for PPMS chains, one should also expect to find more than a single adhesive minimum. Our efforts to find attractive forces at larger PPMS film thickness were unsuccessful, however.

In seeking to explain the observations, another line of explanation might reason from the irregular shape of the

(32) For a review, see: Israelachvili, J. N. *Intermolecular and Surface Forces*, 2nd ed.; Academic Press: New York, 1992; and references therein.

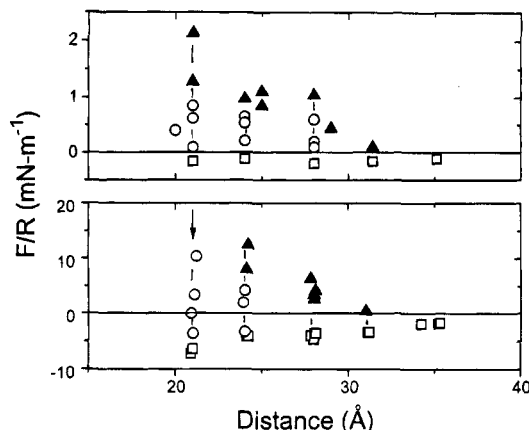


Figure 4. Oscillatory force–distance profile measured for undecane confined between OTE surfaces. Force is normalized by radius of curvature, R , of the crossed mica cylinders. The asymmetry of attractive and repulsive forces may stem from surface deformations induced by repulsion.^{34,35} Triangles (circles) indicate points measured upon squeezing (pulling) the plates together (apart). Squares indicate the force at which the plates jump apart.

atactic PPMS chains—so irregular that these chains refuse to crystallize, but only form glasses at low temperature.²⁴ It has been proposed that oscillations in the force curve vanish when the molecular shape is irregular.³⁶ What constitutes a regular or irregular shape remains poorly understood, however, so it is difficult to assess the validity of this line of argument to explain the absence of observable oscillatory forces in the PPMS system. The possibility that irregular packing played an essential part in the physical picture is given credence by the findings for shear of polymer A, discussed below.

Still another conceivable interpretation of these forces is in terms of van der Waals forces and surface energy. By the JKR approximation,³² the level of adhesion in Figure 3 corresponds to a surface energy of 1 mJ m^{-2} , perhaps not an unreasonable value for this partially-wetting situation. But if these adhesive forces reflected solely van der Waals forces, equilibration during these measurements should not have been so sluggish. In particular, the depth of the adhesive minima depended upon the time waited for equilibration during separation. When the time per datum was less than 10 min, we found the adhesive minimum to be deeper than indicated in Figure 3. Thus van der Waals forces may have contributed to the adhesion but cannot fully explain it.

Parenthetically, we note that the time necessary for equilibration during separation is expected to be longer when the film thickness is increased than when it is compressed, since the relevant relaxation time is now that of the confined liquid, which will be shown below to be many orders of magnitude greater than that of the bulk.

In conclusion, the most likely possibility appears to be that adhesion resulted from the bridging of polymer chains between the OTE layers, so that chains became attached to both surfaces at once.

Thickness Dependence of Dynamic Shear Forces.

We now turn to the dynamic oscillatory shear forces. These, it emerged, were below the experimental resolution except in the region of finite surface forces.

Figure 5 illustrates plots of the changes of dynamic shear forces (at 1 Hz) as the static force, resisting compression

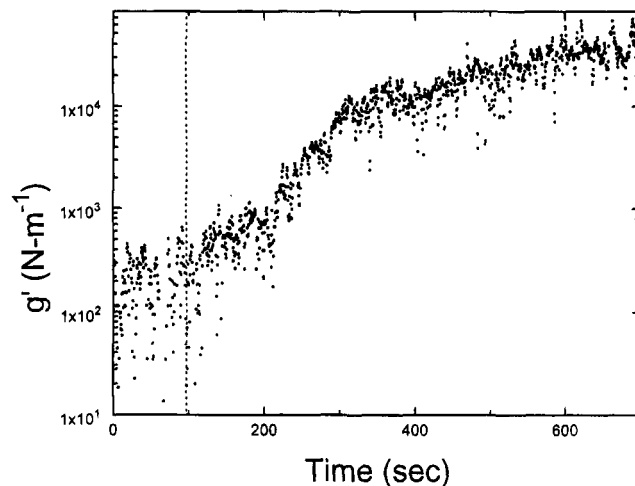


Figure 5. Elastic force component g' at 1 Hz plotted against elapsed time (no signal averaging) as OTE surfaces, separated by polymer D, moved into contact from $\approx 21 \text{ \AA}$ thickness from thermal drift at a rate of $\approx 1 \text{ \AA s}^{-1}$. Note that solidification appeared to be a continuous process. Dotted line indicates $D = 21 \text{ \AA}$.

of the film, was increased. Here the shear forces were measured in real time (without signal averaging) as OTE surfaces, separated by polymer D, moved closer and closer together because of slow thermal drifts in the dimensions of the apparatus. It is striking that the transition to a measurable shear force took place at a film thickness 21 \AA but appeared to take place continuously in time.

A note concerning the presentation of this data: Because these experiments at $F/R = 0$ involved the shear of crossed cylindrical surfaces, rather than parallel plates,^{8,30} for the reasons discussed in the Experimental Section, it was not possible to normalize the shear forces by the area of contact.

Therefore the measured in-phase (elastic) and out-of-phase (viscous) forces at each frequency (ω) were normalized by strain only. This gave an effective spring constant, designated $g'(\omega)$, and an effective loss constant, designated $g''(\omega)$. For qualitative comparison with the conventional storage and loss shear moduli, $G'(\omega)$ and $G''(\omega)$, it is instructive to note the following. First, in measurements which did involve parallel plates,^{8,30} the measured contact area did not change with oscillation frequency. Thus, the differences between g' and G' (elasticity), and g'' and G'' (dissipation), are expected to be a constant factor in any experiment, and their frequency dependence is expected to be the same.

Second, one can estimate that the magnitude of G' was approximately 10 times that of g' , and similarly for G'' and g'' , as described below in eqs 1 and 2. In some experiments the shear measurements were made first (at small compressive force) between crossed cylinders and then (at large compressive force) between parallel plates, and this general qualitative relation was validated. The above estimate follows from the definition of the shear moduli between parallel plates:

$$G' = (h/A)g' \quad (1)$$

$$G'' = (h/A)g'' \quad (2)$$

recognizing that the effective area of contact between the crossed cylinders³² was $A \approx 10^{-10} \text{ m}^{-2}$ and that the polymer film thickness was $h \approx 17 \text{ \AA}$.

The limit of experimental resolution was then $G'(\omega)$ and $G''(\omega) \approx 10^3 \text{ Pa}$, indicating that smaller moduli could

(33) Demirel, A. L.; Reiter, G.; Granick, S. *Science* **1994**, *263*, 1741.

(34) Parker, J. L.; Attard, P. *J. Phys. Chem.* **1992**, *96*, 10398.

(35) Christenson, H. K.; Yaminsky, V. V. *Langmuir* **1993**, *9*, 2448.

(36) Israelachvili, J. N.; Kott, S. J.; Gee, M.; Witten, T. *Macromolecules* **1989**, *22*, 4247.

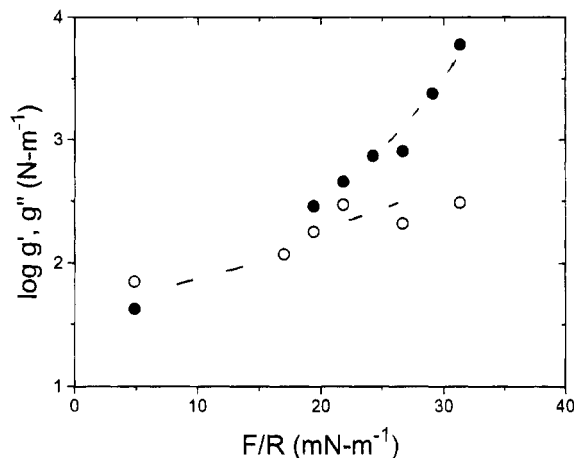


Figure 6. Data for polymer A. Shear elastic constant g' (filled circles) and loss constant g'' (hollow circles) measured at 1 Hz, plotted on a logarithmic scale against the repulsive static force in the normal direction.

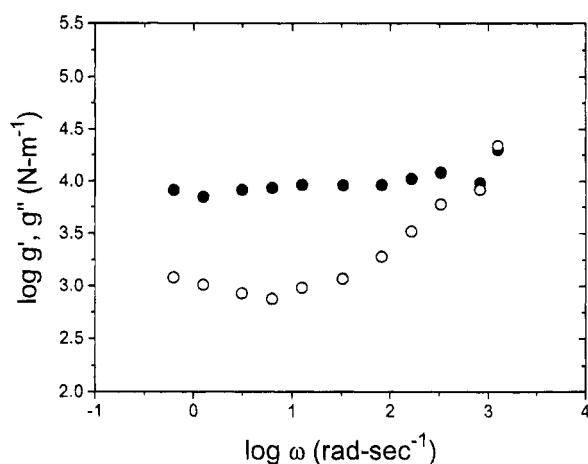


Figure 7. Data for polymer A. Log-log plot of elastic constant g' (filled circles) and loss constant g'' (hollow circles), as a function of angular frequency of measurement, ω , at thickness $17 \pm 2 \text{ \AA}$.

not have been detected in these experiments which were performed at small strains.

Polymer A. This polymer, the lowest molecular weight sample studied ($M_n = 2240$), showed no measurable dynamic shear forces except when highly compressed. The monotonic increase of the elastic and dissipative shear constants with increasing compression is illustrated in Figure 6 for data measured at 1 Hz. Below $F/R \approx 5 \text{ mN/m}$, the shear moduli measured in the region of linear response were below the limit for experimental detection.

This contrasts sharply with the shear rheology of short linear alkanes confined between OTE surfaces. In particular, confined undecane (C_{11}) presents prominent viscoelastic anomalies at several molecularly-thin film thicknesses at which $F/R = 0.33$. This difference from the behavior of polymer A lends credence to the argument, advanced above, of the significance for these experiments of PPMS's irregular shape.

The frequency dependence of the shear response at large compression was also measured. In Figure 7, $g'(\omega)$ and $g''(\omega)$ of a film $17 \pm 2 \text{ \AA}$ thick, at 4.5 MPa normal pressure, are plotted against radian frequency, ω , on logarithmic axes. One notes that $g'(\omega) > g''(\omega)$ except at the highest frequencies and that $g'(\omega)$ was virtually independent of frequency. In connection with polymer C (see below),

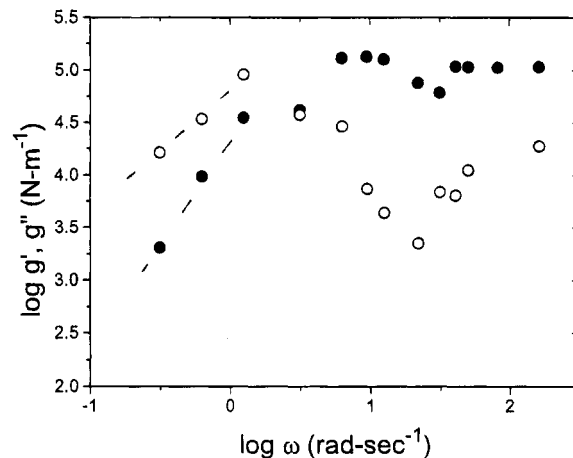


Figure 8. Data for polymer B. Log-log plot of elastic constant g' (filled circles) and loss constant g'' (hollow circles), as a function of angular frequency of measurement, ω , at thickness $17 \pm 2 \text{ \AA}$.

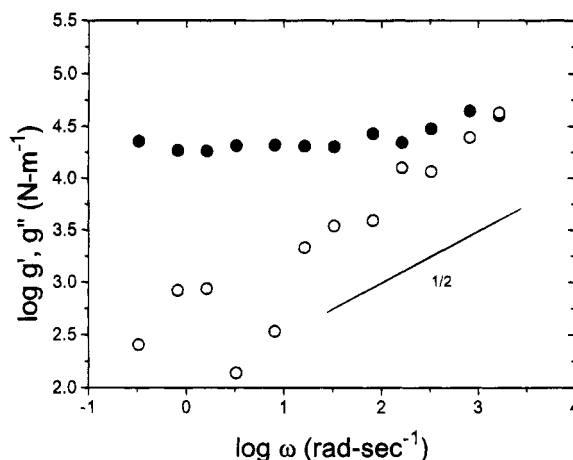


Figure 9. Data for polymer C sheared between parallel plates (rather than crossed cylinders). Area of contact, $3 \times 10^{-10} \text{ m}^2$. Log-log plot of elastic constant g' (filled circles) and loss constant g'' (hollow circles) as a function of angular frequency of measurement, ω , at thickness $17 \pm 2 \text{ \AA}$. A line of slope $1/2$ is drawn as a guide to the eye.

quantitative aspects of this predominantly elastic response are discussed.

Polymer B. The shear dynamics were slower than for polymer A, and shear forces were large enough to be measured, in the hard-wall region, even at $F/R = 0$. In Figure 8, $g'(\omega)$ and $g''(\omega)$ of a film $17 \pm 2 \text{ \AA}$ thick are plotted against radian frequency on logarithmic axes.

The data split into two regimes: low frequencies, where $g'(\omega)$ and $g''(\omega)$ are comparable in magnitude, and higher frequencies, where $g'(\omega)$ exceeds $g''(\omega)$. The inverse frequency at the split defines a relaxation time of the system, approximately 2 s. Qualitatively, the data in Figure 8 resemble the classical viscoelastic behavior of high molecular weight polymer fluids at the transition between terminal and plateau zones.³¹

One notes that these data are essentially the same as we observed previously for this same PPMS sample between freshly-cleaved mica surfaces.⁸ In that case the strongly-adsorbing surface gave comparable data at the much larger PPMS film thickness of 62 \AA ($4.8R_G$), however.

Polymer C. In Figure 9, $g'(\omega)$ and $g''(\omega)$ of a film of polymer C ($M_n = 10\,600$), $17 \pm 2 \text{ \AA}$ thick, are plotted against radian frequency on logarithmic axes.

As some of these measurements were performed with flattened surfaces, Figure 10 shows the same data as in

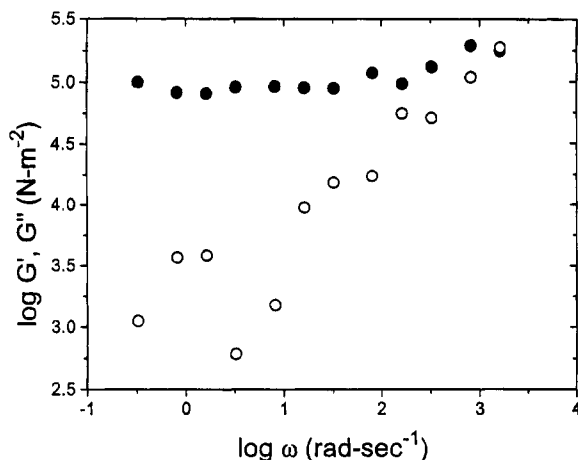


Figure 10. Same data as in Figure 9 but normalized by the film thickness and measured area of contact (eqs 1 and 2) to give the storage and loss shear moduli, storage modulus (filled circles) and loss modulus (hollow circles), $G'(\omega)$ and $G''(\omega)$, respectively. The moduli are plotted on log-log scales against the angular frequency of measurement.

Figure 9 but represented in terms of the storage and loss shear moduli, $G'(\omega)$ and $G''(\omega)$. Comparison of these two representations of the same data supports the conclusions discussed above regarding the respective magnitudes of g' and g'' , and G' and G'' .

This polymer of higher molecular weight displayed still slower relaxation than polymers A and B at this same compression. One notes that $g'(\omega)$ ($\approx 2 \times 10^4$ N m $^{-1}$) showed minimal dependence on the frequency of deformation. Estimated as a storage modulus as discussed above, this is consistent with the storage modulus measured between freshly cleaved mica.^{8,30}

The loss modulus in Figure 9 is also informative. This was an order of magnitude less than the storage modulus except at the highest frequency, where $g'(\omega)$ crossed $g''(\omega)$. However, $g''(\omega)$ at low frequency increased much more slowly than proportionally to the frequency; the data are consistent, over several decades of frequency, with the relation $g'' \propto \omega^{1/2}$.

The scatter of the data at the lowest frequencies makes it difficult to determine whether g'' continues to decrease or levels off with decreasing ω . We suggest tentatively that, at still lower frequencies, g'' would increase and eventually pass through a maximum, as in Figure 8. Unfortunately, these lower frequencies were not accessible experimentally.

In contrast to polymer A, no dependence was found on the magnitude of compressive forces. It seems that polymer A became solidified partially by application of compressive forces but that for polymers B and C the solidification was produced solely by confinement.

Discussion and Conclusions

We emphasize, above all, the qualitative agreement between these measurements of PPMS chains confined between weakly adsorbing surfaces and measurements

previously presented^{8,30} of PPMS confined between strongly adsorbing surfaces. The general conclusion of slowing down of near-surface dynamics appears to hold regardless of the strength of surface adsorption.

A few words are in order regarding the observation that these liquid films, placed between nonadsorbing walls, did not collapse to zero thickness. On the contrary, theory, simulation, and experiment all agree that the structural forces of a liquid exist even between nonadsorbing walls: the fundamental reason is that structural forces are analogous to the radial distribution function that characterizes even hard-sphere liquids in the bulk.³⁷ Complete expulsion of fluid from between two solid surfaces should not be expected.

On the quantitative side, it is also interesting to consider the magnitudes of the relaxation times inferred from these measurements. The bulk viscosity of PPMS of these short chain lengths is low (≈ 100 Pa s),⁸ indicating a rapid longest relaxation time of order 1–10 μ s.³¹ Consequently, in bulk samples, the elastic response should be far less than the dissipative response. In contrast, Figure 8 indicates a relaxation time of 2 s. In Figure 9, the longest relaxation time was even slower, below the lowest accessible experimental frequency.

A provocative point is that the confined polymer films were scarcely thicker than a monolayer per surface. Explanation of the extreme slowing down of the longest shear rheological relaxation time, with increasing molecular weight, in these nearly two-dimensional films, should be pursued in further work.

We consider the static force measurements presented here to be definitive. But it cannot yet be definitively excluded that the observed slowing down of the shear rheological relaxation times, compared with the bulk, might somehow stem from the influence of flaws within the OTE monolayers. We are not aware of a mechanism by which flaws would produce these effects, however. In addition, it would seem an odd coincidence that flaws would generate shear responses quantitatively so similar to those also observed for these same polymers confined between freshly-cleaved mica. We conclude that the slowing down of near-surface dynamics appears likely to result essentially from geometrical confinement.

Experiments are in progress with polymers of other architecture (ring-linear comparisons), and other chemical compositions above and below the entanglement molecular weight, to explore these questions experimentally.

Acknowledgment. We thank K. S. Schweizer for discussions, S. J. Clarson for donating polymer samples, and H.-W. Hu for the force-distance profile between mica surfaces. S.G. acknowledges support from Grant NSF-MSS-92-02143 and the Exxon Corp. for generous financial assistance. At the University of Illinois, we acknowledge support of the National Science Foundation through the Materials Research Laboratory at the University of Illinois, Grant NSF-DMR-89-20538.

(37) Walley, K. P.; Schweizer, K. S.; Peanasky, J.; Cai, L. L.; Granick, S. *J. Chem. Phys.* **1994**, *100*, 3361.